PHYSICAL REVIEW B **81**, 060504(R) (2010)

Structure of neutron-scattering peaks in both s_{++}-wave and $s_{\pm}$-wave states of an iron pnictide superconductor

Seiichiro Onari,[1] Hiroshi Kontani,[2] and Masatoshi Sato[2]
[1]*Department of Applied Physics and JST-TRIP, Nagoya University, Furo-cho, Nagoya 464-8602, Japan*
[2]*Department of Physics and JST-TRIP, Nagoya University, Furo-cho, Nagoya 464-8602, Japan*
(Received 28 December 2009; revised manuscript received 28 January 2010; published 16 February 2010)

We study the neutron-scattering spectrum in iron pnictides based on the random-phase approximation in the five-orbital model for fully gapped s-wave states with sign reversal ($s_{\pm}$) and without sign reversal (s_{++}). In the s_{++}-wave state, we find that a prominent hump structure appears just above the spectral gap by taking account of the quasiparticle damping γ due to strong electron-electron correlation: as the superconductivity develops, the reduction in γ gives rise to the large overshoot in the spectrum above the gap. The obtained hump structure looks similar to the resonance peak in the $s_{\pm}$-wave state, although the height and weight of the peak in the latter state is much larger. In the present study, experimentally observed broad spectral peak in iron pnictides is naturally reproduced by assuming the s_{++}-wave state.

DOI: 10.1103/PhysRevB.81.060504 PACS number(s): 74.20.Rp, 74.20.Fg, 74.25.Dw, 78.70.Nx

Since the discovery of superconductivity in iron pnictides with high transition temperature (T_c) next to high-T_c cuprates,[1] the structure of the superconducting (SC) gap has been studied very intensively. The SC gap in many iron pnictides is fully gapped and band dependent, as shown by the penetration depth measurement[2] and the angle-resolved photoemission spectroscopy (ARPES),[3,4] except for P-doped Ba122.[5] The fully gapped state is also supported by the rapid suppression in $1/T_1(\propto T^n; n\sim 4-6)$ below T_c.[6–8]

In iron pnictides, the nesting of the Fermi surface (FS) between hole and electron pockets is expected to induce the antiferromagnetic (AF) fluctuations in doped metal compounds. Since fully gapped sign-reversing s-wave state ($s_{\pm}$-wave state) is a natural candidate,[9,10] it is urgent to clarify the sign reversal in the SC gap via phase-sensitive experiments. One of the promising methods is the neutron-scattering measurement: existence of the resonance peak at a nesting wave vector $\mathbf{Q}$ is a strong evidence for AF fluctuation mediated superconductors with sign reversal.[11–13] The resonance condition is $\omega_{\rm res} < 2\Delta$, where $\omega_{\rm res}$ is the resonance energy and Δ is magnitude of the SC gap at $T=0$. The resonance peak has been observed in many AF fluctuation mediated unconventional superconductors, such as high-T_c cuprates,[14–16] $CeCoIn_5$,[17] and UPd_2Al_3.[18]

Neutron-scattering measurements for iron pnictides have been performed[19–22] after the theoretical predictions.[23,24] Although clear peak structure was observed in $FeSe_{0.4}Te_{0.6}$ (Ref. 20) and $BaFe_{1.85}Co_{0.15}As_2$,[21] its weight is much smaller than that in high-T_c cuprates and $CeCoIn_5$, and the resonance condition $\omega_{\rm res} < 2\Delta$ is not surely confirmed, as we will discuss later.

Nonmagnetic impurity effect also offers us useful phase-sensitive information. Theoretically, $s_{\pm}$-wave state should be very fragile against impurities due to the interband scattering;[25] the predicted critical residual resistivity $\rho_{\rm imp}^{\rm cr}$ for vanishing T_c is about 20 $\mu\Omega$ cm. However, experimental $\rho_{\rm imp}^{\rm cr}$ reaches $\sim$750 $\mu\Omega$ cm, which corresponds to the minimum metallic conductivity $4e^2/h$ per layer.[26] Since this result supports a conventional s-wave state without sign reversal (s_{++}-wave state), we have to resolve the discrepancy between neutron-scattering measurements and the impurity effects.

In this Rapid Communication, we study the dynamical spin susceptibility $\chi^s(\omega, \boldsymbol{Q})$ based on the five-orbital model[10] for both s_{++}- and $s_{\pm}$-wave states and discuss by which pairing state the experimental results are reproducible. In the normal state, $\chi^s(\omega, \boldsymbol{Q})$ is strongly suppressed by the quasiparticle damping γ due to strong correlation. However, this suppression diminishes in the SC state since γ is reduced as the SC gap opens. For this reason, a prominent hump structure *unrelated to the resonance mechanism* appears in $\chi^s(\omega, \boldsymbol{Q})$ just above 2Δ in the s_{++} wave state. In the $s_{\pm}$-wave state, very high and sharp resonance peak appears at $\omega_{\rm res} < 2\Delta$. We demonstrate that the broad spectral peak observed in iron pnictides is naturally reproduced based on the s_{++}-wave state rather than the $s_{\pm}$-wave state.

Now, we study the 10×10 Nambu BCS Hamiltonian $\hat{\mathcal{H}}_{\boldsymbol{k}}$ composed of the five-orbital model introduced in Ref. 10 and the singlet SC gap.[25] The FSs are shown in Fig. 1(a). The 10×10 Green's function is given by

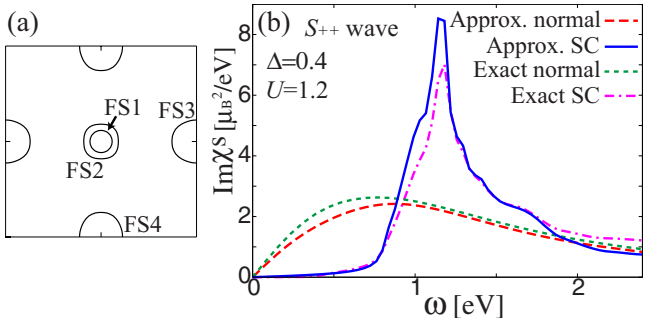

FIG. 1. (Color online) (a) FSs in iron pnictides. (b) ω dependence of Im $\chi^s(\omega, \boldsymbol{Q})$ for the s_{++}-wave state ($\Delta=0.4$) and the normal state at $T=0.01$. The "exact result" is obtained by Eq. (2) using 256^2 $\boldsymbol{k}$-meshes and 1000 x meshes. The "approximate result" is obtained by Eq. (6) using 1024^2 $\boldsymbol{k}$ meshes. We put $a(\epsilon)=0.05$ for $|\epsilon| < 3\Delta$.

$$\hat{\mathcal{G}}(i\omega_n,\boldsymbol{k}) \equiv \begin{pmatrix} \hat{G}(i\omega_n,\boldsymbol{k}) & \hat{F}(i\omega_n,\boldsymbol{k}) \\ \hat{F}^{\dagger}(i\omega_n,\boldsymbol{k}) & -\hat{G}(-i\omega_n,\boldsymbol{k}) \end{pmatrix}^{-1}$$
$$= (i\omega_n\hat{1} - \hat{\Sigma}_{\boldsymbol{k}}(i\omega_n) - \hat{\mathcal{H}}_{\boldsymbol{k}})^{-1}, \quad (1)$$

where $\omega_n = \pi T(2n+1)$ is the fermion Matsubara frequency, $\hat{G}$ ($\hat{F}$) is the 5×5 normal (anomalous) Green's function, and $\hat{\Sigma}_{\boldsymbol{k}}$ is the self-energy in the d-orbital basis. For a while, we assume that the SC gap for the αth FS is band independent; $|\Delta_\alpha| = \Delta$. Hereafter, the unit of energy is eV, unless otherwise noted.

Here, we have to obtain the spin susceptibility as function of real frequency. For this purpose, it is rather easy to use the Matsubara frequency method and the numerical analytic continuation (pade approximation). In the present study, however, we perform the analytical continuation before numerical calculation to obtain more reliable results. The irreducible spin susceptibility in the singlet SC state is given by[13]

$$\hat{\chi}^{0\mathrm{R}}_{l_1l_2,l_3l_4}(\omega,\boldsymbol{q}) = \frac{1}{N}\sum_{\boldsymbol{k}}\int\frac{dx}{2}$$
$$\left\{\tanh\frac{x}{2T}[G^{\mathrm{R}}_{l_1l_3}(k_+)\rho^{\mathrm{G}}_{l_4l_2}(k) + F^{\mathrm{R}}_{l_1l_4}(k_+)\rho^{\mathrm{F}\dagger}_{l_3l_2}(k)]\right.$$
$$\left. + \tanh\frac{x_+}{2T}[\rho^{\mathrm{G}}_{l_1l_3}(k_+)G^{\mathrm{A}}_{l_4l_2}(k) + \rho^{\mathrm{F}}_{l_1l_4}(k_+)F^{\dagger\mathrm{A}}_{l_3l_2}(k)]\right\}, \quad (2)$$

where $x_+ = x+\omega$, $\boldsymbol{k}_+ = \boldsymbol{k}+\boldsymbol{q}$, and $k_{(+)} = (x_{(+)}, \boldsymbol{k}_{(+)})$. $l_i = 1\sim5$ represents the d orbital, and A (R) represents the advanced (retarded) Green's function. $\rho^{\mathrm{G}}_{ll'}(k) \equiv (G^{\mathrm{A}}_{ll'}(k) - G^{\mathrm{R}}_{ll'}(k))/(2\pi i)$ and $\rho^{\mathrm{F}(\dagger)}_{ll'}(k) \equiv (F^{(\dagger)\mathrm{A}}_{ll'}(k) - F^{(\dagger)\mathrm{R}}_{ll'}(k))/(2\pi i)$ are one-particle spectral functions. Since $\rho^{\mathrm{G,F}}_{ll'}(k) = 0$ for $|x| < \Delta$, Im $\hat{\chi}^{0\mathrm{R}}(\omega,\boldsymbol{q}) = 0$ for $|\omega| < 2\Delta$. That is, the particle-hole excitation gap is 2Δ.

Then, the spin susceptibility $\chi^s(\omega,\boldsymbol{q})$ is given by the multiorbital random-phase approximation (RPA) with the intraorbital Coulomb U, the interorbital Coulomb U', the Hund coupling J, and the pair-hopping J',[10]

$$\chi^s(\omega,\boldsymbol{q}) = \sum_{i,j}\left[\frac{\hat{\chi}^{0\mathrm{R}}(\omega,\boldsymbol{q})}{1-\hat{S}^0\hat{\chi}^{0\mathrm{R}}(\omega,\boldsymbol{q})}\right]_{ii,jj}, \quad (3)$$

where vertex of spin channel $\hat{S}^0_{l_1l_2,l_3l_4} = U$, U', J, and J' for $l_1=l_2=l_3=l_4$, $l_1=l_3\neq l_2=l_4$, $l_1=l_2\neq l_3=l_4$, and $l_1=l_4\neq l_2=l_3$, respectively. Hereafter, we put $J=J'=0.15$, $U'=U-2J$, and $U=1\sim1.3$ and fix the electron number as 6.1 (10% electron-doped case). In the present model, $\chi^s(0,\boldsymbol{q})$ takes the maximum value when $\boldsymbol{q}$ is the nesting vector $\boldsymbol{Q}=(\pi,\pi/16)$. Due to the nesting, $\chi^s(0,\boldsymbol{Q})/\chi^0(0,\boldsymbol{Q}) \approx 1/(1-\alpha_{\mathrm{St}})$ is enhanced; α_{St} ($\lesssim1$) is the maximum eigenvalue of $\hat{S}^0\hat{\chi}^{0\mathrm{R}}(0,\boldsymbol{Q})$ that is called the Stoner factor.

In strongly correlated systems, $\chi^s(\omega,\boldsymbol{q})$ is renormalized by the self-energy correction. In nearly AF metals, for example, the temperature dependence of the self-energy induces the Curie-Weiss behavior of $\chi^s(0,\boldsymbol{Q})$. At the moment, there is no experimental information on the $\boldsymbol{k}$, ϵ, and band dependences of the self-energy. Therefore, we phenomenologically introduce a band-diagonal self-energy as $\hat{\Sigma}^{\mathrm{R}}_{\boldsymbol{k}}(\epsilon) = i\gamma(\epsilon)\hat{1}$. First, we estimate the value of $\gamma(\epsilon)$ in the normal state. Since the conductivity is given by $\sigma = e^2\Sigma_\alpha N_\alpha(0)v^2_\alpha/2\gamma(0)$, where $N_\alpha(0)$ and v_α are the density of states (DOS) and the Fermi velocity of the αth FS, we obtain $\rho \approx (2\gamma[\mathrm{meV}])\ \mu\Omega$ cm.[25] Since $\rho(T)-\rho(0) \sim (5T[\mathrm{meV}])\ \mu\Omega$ cm in $BaFe_{1.84}Co_{0.16}As_2$ below 100 K,[27] $\gamma(0)$ due to inelastic scattering is estimated as $2.5T$ which is comparable to that in overdoped cuprates. If we assume the relation $\gamma(\epsilon) \propto (\pi T+\epsilon)$ in nearly AF Fermi liquid,[28] we obtain $\gamma(\epsilon) \sim 2.5(T+\epsilon/\pi)$.

Now, we calculate Im $\chi^s(\omega,\boldsymbol{Q})$ in both normal and s_{++}-wave SC states, concentrating on the frequency $\omega \sim 2\Delta$. To estimate the renormalization of Im $\chi^s(\omega,\boldsymbol{Q})$ due to the self-energy, we have to know the value of $\gamma(\epsilon)$ with $|\epsilon| \sim \Delta$ in both normal and SC states. Considering that $\gamma(\epsilon) = 2.5(T+\epsilon/\pi) \sim 2\Delta$ at $T_c = 2.2$ meV and $\epsilon = \Delta \sim 5$ meV in $BaFe_{1.85}Co_{0.15}As_2$, in the present study, we simply put $\gamma(\epsilon)$ in the normal state at T_c as

$$\gamma(\epsilon) = \gamma_0 \quad (4)$$

with $\gamma_0 \gtrsim \Delta$. In the present model, $\alpha_{\mathrm{St}} = 0.84(0.79)$ for $U = 1.3(1.2)$ when $\gamma_0 = 0.1$ and $T = 0.002$; the T dependence of α_{St} is small when γ_0 is fixed.

In the SC state at $T \ll T_c$, $\gamma(\epsilon) = 0$ for $|\epsilon| < 3\Delta$ (=particle-hole excitation gap 2Δ plus one-particle gap Δ),[12] and its functional form is approximately the same as that in the normal state for $|\epsilon| \gtrsim 3\Delta$. Then, we put

$$\gamma(\epsilon) = a(\epsilon)\gamma_s \quad (5)$$

where (i) $a(\epsilon) \ll 1$ for $|\epsilon| < 3\Delta$, (ii) $a(\epsilon) = 1$ for $|\epsilon| > 4\Delta$, and (iii) linear extrapolation for $3\Delta < |\epsilon| < 4\Delta$. We have confirmed that the obtained results are insensitive to the boundary of $|\epsilon|$ (4Δ in the present case) between (ii) and (iii). Although γ_s at $T \ll T_c$ should be smaller than γ_0 at $T = T_c$, we simply put $\gamma_s = \gamma_0$ hereafter, which causes underestimation of the peak height of Im χ^s.

Figure 1 shows Im $\chi^s(\omega,\boldsymbol{Q})$ obtained by Eqs. (2) and (3) for $U = 1.2$. We put $\Delta = \gamma_0 = 0.4$ since a reliable calculation of Eq. (2) in the five-orbital model is very numerically demanding for experimental values $\Delta \sim \gamma \sim 0.01$. In the normal state, Im $\chi^s(\omega,\boldsymbol{Q})$ is suppressed by large damping $\gamma_0 \sim \Delta$. In the SC state, the gap in Im $\chi^s(\omega,\boldsymbol{Q})$ is 2Δ. Considering that the particle or hole with energy $|\epsilon| < 3\Delta$ is free from inelastic scattering in the SC state, the lifetime of particle-hole excitation with energy $|\epsilon| < 4\Delta$ should be very long below T_c. For this reason, Im $\chi^s(\omega,\boldsymbol{q})$ shows a large hump structure for $2\Delta \lesssim \omega \lesssim 4\Delta$ in the s_{++}-wave state.

As discussed above, we cannot use smaller Δ and γ in calculating Eq. (2) due to the difficulty of numerical computation. To solve this problem, we perform the x integration in Eq. (2) approximately as follows: when $\hat{\gamma} = \gamma\hat{1}$, the retarded (advanced) 10×10 Green's function is expressed as $\hat{\mathcal{G}}^{\mathrm{R(A)}}_{m,m'}(x,\boldsymbol{k}) = \Sigma_\alpha U^{m,\alpha}_{\boldsymbol{k}}(x+(-)i\gamma - E^\alpha_{\boldsymbol{k}})^{-1}U^{m',\alpha^*}_{\boldsymbol{k}}$, where $E^\alpha_{\boldsymbol{k}}$ ($\alpha = 1\sim10$) is the eigenvalue of $\hat{\mathcal{H}}_{\boldsymbol{k}}$ and $\hat{U}_{\boldsymbol{k}}$ is the corresponding unitary matrix. We promise that $E^\alpha_{\boldsymbol{k}} = -E^{\alpha+5}_{\boldsymbol{k}}$

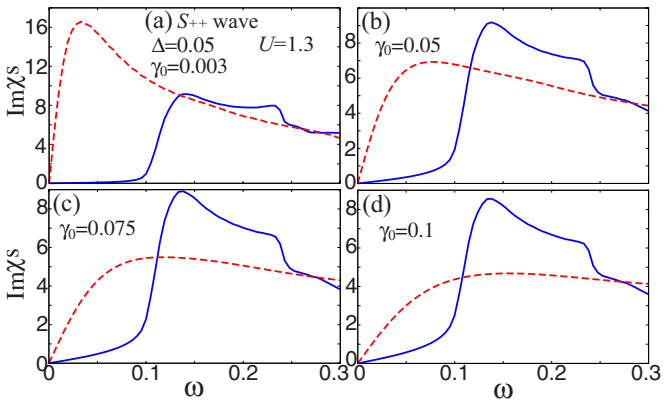

FIG. 2. (Color online) Obtained Im $\chi^s(\omega,\boldsymbol{Q})$ in the s_{++}-wave (solid line) and normal (broken line) states for $\gamma_0<0.1$, using 1024^2 $\boldsymbol{k}$ meshes. We put $a(\epsilon)=0.003/\gamma_0$ for $|\epsilon|<3\Delta$.

for $1\leq\alpha\leq5$. When γ is sufficiently small, then $\rho_{ll'}^{\mathrm{G(F)}}(x,\boldsymbol{k})\approx\Sigma_\alpha U_{\boldsymbol{k}}^{l,\alpha}\delta(x-E_{\boldsymbol{k}}^{\alpha})U_{\boldsymbol{k}}^{l'(+5),\alpha^*}$, and thus Eq. (2) becomes

$$\hat{\chi}^{0\mathrm{R}}_{l_1l_2,l_3l_4}(\omega,\boldsymbol{q})\approx\frac{1}{N}\sum_{\boldsymbol{k}}\sum_{l,l'}\frac{f(E_{\boldsymbol{k}}^{l})-f(E_{\boldsymbol{k}+\boldsymbol{q}}^{l'})}{\omega+E_{\boldsymbol{k}}^{l}-E_{\boldsymbol{k}+\boldsymbol{q}}^{l'}+i\Gamma_{ll',\boldsymbol{kq}}}$$

$$[U_{\boldsymbol{k}+\boldsymbol{q}}^{l_1,l'}U_{\boldsymbol{k}+\boldsymbol{q}}^{l_3,l'^*}U_{\boldsymbol{k}}^{l_4l}U_{\boldsymbol{k}}^{l_2l^*}+U_{\boldsymbol{k}+\boldsymbol{q}}^{l_1,l'}U_{\boldsymbol{k}+\boldsymbol{q}}^{l_4+5,l'^*}U_{\boldsymbol{k}}^{l_3+5,l}U_{\boldsymbol{k}}^{l_2l^*}],\qquad(6)$$

with $\Gamma_{ll',\boldsymbol{kq}}=\gamma$ for $\gamma\ll1$.

When γ is as large as Δ, however, we have to check to what extent Eq. (6) is reliable. Considering that the origin of the renormalization of χ^s is the quasiparticle damping $\gamma(E_{\boldsymbol{k}}^{l})$ and $\gamma(E_{\boldsymbol{k}+\boldsymbol{q}}^{l'})$, we introduce the following approximation:

$$\Gamma_{ll',\boldsymbol{kq}}=b\cdot\max\{\gamma(E_{\boldsymbol{k}}^{l}),\gamma(E_{\boldsymbol{k}+\boldsymbol{q}}^{l'})\}\qquad(7)$$

where $b\approx1$ is a fitting parameter. $\Gamma_{ll',\boldsymbol{kq}}\approx0$ in the SC state for $|E_{\boldsymbol{k}}^{l}|,|E_{\boldsymbol{k}+\boldsymbol{q}}^{l'}|<3\Delta$, reflecting the absence of quasiparticle damping. In Fig. 1, we show numerical results given by the present approximation with $b=1.3$; we replace $b\gamma_0$ with γ_0 hereafter since $b\approx1$. Since the "exact results" given by Eq. (2) is quantitatively reproduced, we decide to calculate Im $\chi^s(\omega,\mathbf{Q})$ using Eqs. (6) and (7) for more realistic values of Δ and γ. This approximation works well when γ is comparable to or smaller than Δ.

Figure 2 shows Im $\chi^s(\omega,\boldsymbol{Q})$ obtained by Eqs. (6) and (3) for $U=1.3$ and $T=0.002$. We put $\Delta=0.05$ in the s_{++}-wave SC state; although it is a few times larger than the gap for

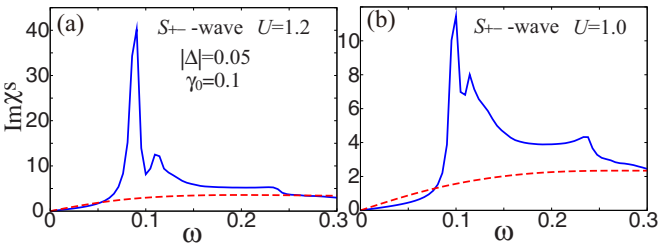

FIG. 4. (Color online) Im $\chi^s(\omega,\boldsymbol{Q})$ for $s_{\pm}$-wave (solid line) and normal (broken line) states, with $U=1.2$ and 1.0. We put $\gamma_0=0.1$ and $a(\epsilon)=0.03$ for $|\epsilon|<3\Delta$.

Sm1111 with $T_c=56$ K, it is enough smaller than the Fermi energies of electron and hole pockets.[10] When (a) $\gamma_0=0.003$, Im $\chi^s(\omega,\boldsymbol{Q})$ in the SC state approximately equal to that in the normal state for $\omega>2\Delta$. As γ_0 increases from (b) 0.05 to (d) 0.1, Im $\chi^s(\omega,\boldsymbol{Q})$ in the normal state decreases gradually, whereas that in the SC state depends on γ_0 only slightly since $\gamma(\epsilon)\approx0$ for $|\epsilon|<3\Delta$. Therefore, in the case of $\gamma_0\gtrsim\Delta$, Im $\chi^s(\omega,\boldsymbol{Q})$ in the SC state shows a prominent hump structure, and its peak value is about double of that in the normal state. In (d), experimental approximate "sum rule" at fixed $\boldsymbol{q}=\boldsymbol{Q}$ (Ref. 21) is well satisfied. In Figs. 2(c) and 2(d), a relatively large slope for $|\epsilon|<2\Delta$ is an artifact of the approximation due to large γ_0/Δ.

Next, we study the effect of band-dependent SC gap observed by ARPES measurements.[3,4] In Fig. 3(a), we put $U=1.3$, $\Delta_{1,2,4}=\Delta_{\max}=0.07$ for FS1, 3, 4, and $\Delta_2=\Delta_{\min}=0.035$ for FS2. Then, Im $\chi^s(\omega,\boldsymbol{Q})$ increases rapidly at $\omega=\Delta_{\max}+\Delta_{\min}=0.105$, and it shows a peak at $\omega=0.14$. In Fig. 3(b), we introduce the anisotropy of the gap function for only FS3 and 4 with ratio 2; $\Delta_{\boldsymbol{k}}=\Delta_{\max}(1-0.5\sin^2\theta_{\boldsymbol{k}})$, where $\theta_{\boldsymbol{k}}=\tan^{-1}[|k_{y(x)}|/(|k_{x(y)}|-\pi)]$ for FS3(4). Then, the peak is located at $\omega=0.125$, which is closer to $\Delta_{\max}+\Delta_{\min}=0.105$. In the case of $\Delta_{\max}\neq\Delta_{\min}$, the reduction in Im $\chi^s(\omega,\boldsymbol{Q})$ by damping occurs for $|\omega|>4\Delta_{\min}$. For this reason, the width of the hump peak in Figs. 3(a) and 3(b) is much sharper than that for the band-independent SC gap in Fig. 2. We have also calculated Im $\chi^s(\omega,\boldsymbol{Q})$ for $\Delta_{3,4}=\Delta_{\max}$ and $\Delta_{1,2}=\Delta_{\min}$ and verified that the obtained result is similar to Fig. 3.

Here, we make comparison with experiments. The peak height and the weight in Fig. 3(b) seems to be consistent with the neutron-scattering measurements in iron pnictides.[19–22] In $BaFe_{1.85}Co_{0.15}As_2$ ($T_c=25$ K), the observed "resonance energy" is $\omega_{\mathrm{res}}=9.5$ meV.[21] According to Ref. 3, $\Delta_{\max}/T_c\approx3.5$ and $\Delta_{\min}/\Delta_{\max}\approx0.35$ in many iron pnictides.

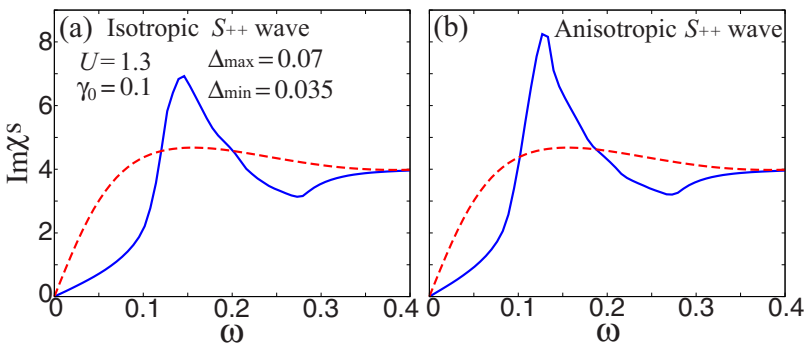

FIG. 3. (Color online) Im $\chi^s(\omega,\boldsymbol{Q})$ for s_{++}-wave (solid line) and normal (broken line) states for $\gamma_0=0.1$, with $\Delta_{\max}=0.07$ and $\Delta_{\min}=0.035$. We put $a(\epsilon)=0.03$ for $|\epsilon|<3\Delta_{\min}$, and $a(\epsilon)=1$ for $|\epsilon|>4\Delta_{\min}$.

(More smaller $\Delta_{\max,\min}$ is reported in Ref. 2.) Thus, $\Delta_{\max}+\Delta_{\min}\approx 4.7T_c=10$ meV is comparable to $\omega_{\rm res}=9.5$ meV in $BaFe_{1.85}Co_{0.15}As_2$. Moreover, finite Im $\chi^s(\omega,\boldsymbol{Q})$ for $\omega\gtrsim 0.3\omega_{\rm res}$ in Ref. 21 may suggest the existence of SC gap anisotropy. Therefore, the theoretical result in Fig. 3(b) is well consistent with experimental data. We note that the hump structure of Im $\chi^s(\omega,\boldsymbol{q})$ for $\boldsymbol{q}=(\pi,0)$ is smaller than that for $\boldsymbol{q}=\boldsymbol{Q}$.

We also analyze the $s_{\pm}$-wave state, where the spin wave without damping, known as the "resonance peak," is expected to emerge at $\omega_{\rm res}<2\Delta$. Figure 4 shows the numerical results for (a) $U=1.2$ and (b) $U=1.0$ in the case of $\Delta_{1,2}=-\Delta_{3,4}=0.05$. In (a), a very sharp and high resonance peak appears at $\omega_{\rm res}=0.85<2\Delta$, consistent with previous theoretical studies.[23,24] Case (b) corresponds to the "heavily overdoped" since $\alpha_{\rm St}=0.69$ and $T_c\sim 0$. The obtained resonance peak in Fig. 4 by taking $\gamma(\epsilon)$ into account is too large to explain experiments even in the case of $\alpha_{\rm St}=0.69$. In clean Y-based high-T_c cuprates, in fact, the observed resonance peak is very sharp and high. Although the resonance peak in Bi-based compounds becomes wider due to the sample inhomogeneity (i.e., nanoscale distribution of T_c),[16] the weight of the peak is ten times larger than that in $BaFe_{1.85}Co_{0.15}As_2$.[21]

In the present study, we have neglected the impurity effect since its influence on $\chi^s(\omega,\boldsymbol{Q})$ is expected to be small. In fact, in the single band model, the reduction in χ^0 due to the impurity self-energy is almost canceled by the impurity vertex correction.[29] Moreover, impurity effect tends to *enhance* $\chi^s(\omega,\boldsymbol{Q})$ in the modified fluctuation exchange approximation in nearly AF metals.[30]

Before closing the study, we shortly discuss the heavy fermion Kondo insulator CeNiSn. As shown in Fig. 1 of Ref. 31, neutron-scattering spectrum at $\boldsymbol{q}=(0,\pi,0)$ in CeNiSn shows a prominent hump peak structure above the hybridization gap below the Kondo temperature T_K, which looks very similar to the spectrum observed in iron pnictides below T_c.[19–22] This hump structure is well reproduced by the dynamical-mean-field theory based on the periodic Anderson model.[32] This fact demonstrates that large hump in Im $\chi^s(\omega,\boldsymbol{Q})$ can appear in strongly correlated systems with one-particle gap, without the necessity of the resonance mechanism.

In summary, we have studied Im $\chi^s(\omega,\boldsymbol{Q})$ in iron pnictides based on the five-orbital model and revealed that a prominent hump structure appears just above 2Δ in the s_{++}-wave state by taking the strongly correlation effect via γ. This hump structure becomes small as α_s decreases in the overdoped region, or $\boldsymbol{q}$ deviates from the nesting vector $\boldsymbol{Q}$. At present, experimental data can be explained in terms of the s_{++}-wave state very well. Further experimental efforts are required to determine the height and width of the "resonance peak" and the magnitude relation between $\omega_{\rm res}$ and $\Delta_{\max}+\Delta_{\min}$.

This study has been supported by Grants-in-Aid for Scientific Research from MEXT of Japan, and by JST, TRIP. Numerical calculations were performed using the facilities of the supercomputer center, ISSP.

[1] Y. Kamihara, T. Watanabe, M. Hirano, and H. Hosono, J. Am. Chem. Soc. **130**, 3296 (2008).
[2] K. Hashimoto *et al.*, Phys. Rev. Lett. **102**, 017002 (2009).
[3] D. V. Evtushinsky *et al.*, New J. Phys. **11**, 055069 (2009).
[4] K. Nakayama *et al.*, EPL **85**, 67002 (2009).
[5] K. Hashimoto, M. Yamashita, S. Kasahara, Y. Senshu, N. Nakata, S. Tonegawa, K. Ikada, A. Serafin, A. Carrington, T. Terashima, H. Ikeda, and T. Shibauchi, and Y. Matsuda, arXiv:0907.4399 (unpublished).
[6] Y. Kobayashi *et al.*, J. Phys. Soc. Jpn. **78**, 073704 (2009).
[7] H. Mukuda *et al.*, J. Phys. Soc. Jpn. **77**, 093704 (2008).
[8] G. Fuchs, S. Drechsler, N. Kozlova, M. Bartkowiak, G. Behr, K. Nenkov, H. Klauss, J. Freudenberger, M. Knupfer, F. Hammerath, G. Lang, H. Grafe, B. Buechner, and L. Schultz, arXiv:0908.2101 (unpublished).
[9] I. I. Mazin, D. J. Singh, M. D. Johannes, and M. H. Du, Phys. Rev. Lett. **101**, 057003 (2008).
[10] K. Kuroki, S. Onari, R. Arita, H. Usui, Y. Tanaka, H. Kontani, and H. Aoki, Phys. Rev. Lett. **101**, 087004 (2008); K. Kuroki, H. Usui, S. Onari, R. Arita, and H. Aoki, Phys. Rev. B **79**, 224511 (2009).
[11] D. K. Morr and D. Pines, Phys. Rev. Lett. **81**, 1086 (1998).
[12] A. Abanov and A. V. Chubukov, Phys. Rev. Lett. **83**, 1652 (1999).
[13] T. Takimoto and T. Moriya, J. Phys. Soc. Jpn. **67**, 3570 (1998).
[14] S. Iikubo *et al.*, J. Phys. Soc. Jpn. **74**, 275 (2005).
[15] M. Ito *et al.*, J. Phys. Soc. Jpn. **71**, 265 (2002).
[16] H. F. Fong *et al.*, Nature (London) **398**, 588 (1999).
[17] C. Stock, C. Broholm, J. Hudis, H. J. Kang, and C. Petrovic, Phys. Rev. Lett. **100**, 087001 (2008).
[18] N. K. Sato *et al.*, Nature (London) **410**, 340 (2001).
[19] A. D. Christianson *et al.*, Nature (London) **456**, 930 (2008).
[20] Y. Qiu *et al.*, Phys. Rev. Lett. **103**, 067008 (2009).
[21] D. Inosov, J. Park, P. Bourges, D. Sun, Y. Sidis, A. Schneidewind, K. Hradil, D. Haug, C. Lin, B. Keimer, and V. Hinkov, arXiv:0907.3632 (unpublished).
[22] J. Zhao, L. Regnault, C. Zhang, M. Wang, Z. Li, F. Zhou, Z. Zhao, and P. Dai, arXiv:0908.0954 (unpublished).
[23] T. A. Maier and D. J. Scalapino, Phys. Rev. B **78**, 020514(R) (2008); T. A. Maier, S. Graser, D. J. Scalapino, and P. J. Hirschfeld, *ibid.* **79**, 224510 (2009).
[24] M. M. Korshunov and I. Eremin, Phys. Rev. B **78**, 140509(R) (2008).
[25] S. Onari and H. Kontani, Phys. Rev. Lett. **103**, 177001 (2009).
[26] M. Sato *et al.*, J. Phys. Soc. Jpn. **79**, 014710 (2010).
[27] A. S. Sefat *et al.*, Physica C **469**, 350 (2009).
[28] B. P. Stojkovic and D. Pines, Phys. Rev. B **56**, 11931 (1997).
[29] N. Bulut, Physica C **353**, 270 (2001).
[30] H. Kontani, Rep. Prog. Phys. **71**, 026501 (2008).
[31] H. Kadowaki *et al.*, J. Phys. Soc. Jpn. **63**, 2074 (1994).
[32] T. Mutou and D. S. Hirashima, J. Phys. Soc. Jpn. **64**, 4799 (1995).